QUANTUM ANTIFERROMAGNETS IN A MAGNETIC FIELD*

B. Normand

Theoretische Physik III, Elektronische Korrelationen und Magnetismus
Universität Augsburg
D-86135 Augsburg, Germany

(Received October 16, 2000)

Low-dimensional antiferromagnets in an external magnetic field provide an ideal illustration of the physics of quantum phase transitions. This theoretical analysis is motivated by the two-leg spin ladder geometry, which has been the subject of much experimental study in the material CuHpCl. The non-linear sigma model is used to characterise the quantum phases of the system, and the bond-operator description to discuss excitation spectra and quantum phase transitions between ground states.

PACS numbers: 75.10.Jm, 75.30.Cr, 75.40.Cx

1. Introduction

Quantum spin systems are those with sufficiently low dimensionality d and spin S that their quantum nature becomes manifest through the effects of fluctuations. Their value in revealing fundamental quantum mechanical properties has been understood since Haldane's conjecture [1] concerning integral- and half-integral-spin AntiFerromagnetic (AF) chains. Application of a magnetic field to such systems affects both the spins and their fluctuations, in ways which can profoundly alter the sample properties, including a change of ground state. Such a process, occurring at zero temperature, is a quantum phase transition [2].

Synthesis of novel metalloorganic materials has provided a range of low-dimensional antiferromagnets in which the small exchange constants permit the full magnetisation to saturation to be measured in laboratory fields. The experimental realisation of many profound features of quantum magnets may be counted as one of the major triumphs of condensed matter physics

* Presented at the XL Cracow School of Theoretical Physics, Zakopane, Poland, June 3–11, 2000.

in the past decade. This overview is intended to highlight some theoretical aspects of the quantum phases and quantum phase transitions which arise in such systems in a magnetic field. The focus will be on the two-chain ladder geometry believed to be appropriate for CuHpCl [3,4] the best-characterised sample in recent literature, but is in fact relevant for a variety of quantum magnets.

CuHpCl provides a weakly-coupled network of $S = {}^1\!/_2$ Cu atoms, which are thought to be most strongly coupled as dimer pairs, with an inter-dimer coupling leading to a configuration of isolated spin ladders. The ratio $\lambda = J'/J \sim 0.2$ of chain to rung couplings (Fig. 1) makes CuHpCl a strongly dimerised system, and as such very well suited to both of the analytical approaches to follow. In an applied magnetic field, magnetisation [3], specific heat [4] and Nuclear Magnetic Resonance (NMR) measurements [5] show clearly the evolution from a gapped system at low field, through a gapless regime at intermediate fields, to a gapped, saturated magnet at high fields. In the terminology of quantum phase transitions [2], these regimes are respectively "quantum disordered", "quantum critical" (an extended regime strictly in one dimension (1d)) and "renormalised classical". More detail will be furnished throughout the text on the meaning of these terms and the properties they describe. A full account of the experiments characterising these phases and realising quantum phase transitions in a field may be found in Ref. [6].

Theoretical studies have been performed using a variety of techniques [7–10]. In the following, Sec. 2 presents the Non-Linear σ Model (NLσM) description [11], which is shown to provide a good, qualitative picture of the quantum phases and their underlying physics. More specific, microscopic results concerning excitation spectra of these phases are obtained in Sec. 3 by employing the bond-operator method, which is found to be ideally suited to discussing quantum phase transitions. Sec. 4 contains a final comparison with experiment and summary.

2. Quantum phases: non-linear σ model

Although the NLσM applies strictly to the semiclassical limit (large S), it has been used frequently as the basis for fundamental deductions about the quantum limit of AF systems. It can be shown to be valid for all effectively integral-spin quantum systems in magnetic fields on the order of the zero-field spin gap. Of the many approaches to this model, a spin stiffness analysis and a renormalisation group technique provide the most appealing description of the broken-symmetry regime of finite magnetisation at intermediate field, and of the low-field regime where symmetry is restored by quantum fluctuations.

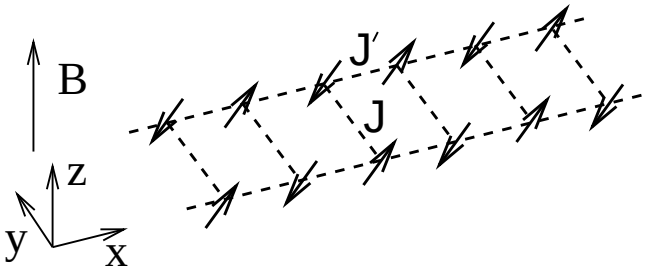

Fig. 1. Schematic representation of two-chain ladder system, with intrachain superexchange coupling J' and interchain coupling J, in applied magnetic field B.

The Hamiltonian for the system (Fig. 1) in a magnetic field $\boldsymbol{b} = \tilde{g}\mu_{\rm B}\boldsymbol{B}$ may be written as

$$H = \sum_{i;m=1,2} \left(J' \boldsymbol{S}_{m,i} \cdot \boldsymbol{S}_{m,i+1} + J \boldsymbol{S}_{1,i} \cdot \boldsymbol{S}_{2,i} + \boldsymbol{b} \cdot \boldsymbol{S}_{m,i} \right). \tag{1}$$

The NLσM action is derived using the coherent-state representation of the spin $\boldsymbol{S}_{m,i}$ as $S\boldsymbol{\Omega}_{m,i} \simeq S[(-1)^{i+m}\boldsymbol{n}_{m,i} + a\boldsymbol{l}_{m,i}]$, where $\boldsymbol{n}_{m,i}$ is the staggered spin, or Néel vector, and the uniform component $\boldsymbol{l}_{m,i}$ describes normal fluctuations. In the continuum limit, the field $\boldsymbol{l}$ is integrated out subject to the constraint $\boldsymbol{l} \cdot \boldsymbol{n} = 0$. A key element of the derivation, which is detailed in full in Ref. [11], is the demonstration that for the two-chain system the Pontryagin index terms for the $S = {}^1\!/_2$ spins are effectively paired due to the finite-size gap across the ladder, placing the ladder in the class of integral-spin systems. Neglecting this term, the action for the quasi-1d system, in $1+1$ Euclidean dimensions denoted by μ, is [12]

$$\mathcal{S}_{\rm E} = \frac{1}{2g} \int d\tau\, dx \, \left\{ (\partial_\mu \boldsymbol{n})^2 - \left[\boldsymbol{b}^2 - (\boldsymbol{n} \cdot \boldsymbol{b})^2 \right] + 2i\boldsymbol{b} \cdot (\boldsymbol{n} \wedge \dot{\boldsymbol{n}}) \right\}, \tag{2}$$

in which $g = (2/N_y S)\sqrt{(J' + \frac{1}{2}J)/J'}$ is the bare coupling constant, and the integral over τ is from zero to $L_{\rm T} = c\beta$, with β the inverse temperature and $c = 2Sa\sqrt{J'(J' + \frac{1}{2}J)}$ the effective spin-wave velocity.

In spherical coordinates for $\boldsymbol{n}$, chosen as $(\vartheta + \pi/2, \phi)$, the corresponding Lagrangean

$$\mathcal{L}_{\rm E} = \frac{1}{2g} \left\{ \left[\left(\dot{\phi} + ib \right)^2 + (\partial_x \phi)^2 \right] - \vartheta \left[\partial_\mu^2 + \left(\dot{\phi} + ib \right)^2 \right] \vartheta \right\} \tag{3}$$

has the physically more transparent form of separating into distinct contributions from in-plane and out-of-plane fluctuations in the high-field regime,

$|b| > \dot{\phi} \equiv \omega$. The field behaves as a hard axis, forcing the spins to align in the normal plane, and can be considered as suppressing out-of-plane fluctuations.

2.1. Spin stiffness

The spin stiffness provides valuable initial insight into the effect of the magnetic field [13]. To 1-loop order in g, this is given by

$$\rho_s = \frac{1}{2} cL \left. \frac{\partial^2 F}{\partial \psi^2} \right|_{\psi=0} = \rho_s^0 \left[1 - \frac{g}{L L_{\mathrm{T}}} \sum_{\boldsymbol{k}} \frac{1}{\boldsymbol{k}^2 + \left(\frac{b}{c}\right)^2} \right], \tag{4}$$

where $\rho_s^0 = c/2g$ is the classical (bare) value, and the sum includes both quantum and thermal (through the finite "length" L_{T}) corrections to first order in g. The system length L over which the stiffness vanishes is the correlation length, which for the quantum regime $L_{\mathrm{T}} \gg L$ is given by

$$\xi(B) = \frac{2L_m^*}{1 - \left(\frac{L_m^*}{L_m}\right)^2} \equiv \frac{\xi_0}{1 - \left(\frac{B}{B^*}\right)^2}. \tag{5}$$

$L_m = \pi c/b$ is the effective magnetic length scale, $\xi_0 = Aa\, \mathrm{e}^{2\pi/g} \propto \mathrm{e}^{\pi S}$ ($A \sim \mathcal{O}(1)$) is the zero-field correlation length familiar from the Haldane analysis, and $L_m^* = a \sinh(2\pi/g)$ gives the critical field B^* at which $\xi(B)$ diverges. For finite fields $B < B^*$, the system has only short-range correlations and finite correlation length (Fig. 2), there is no spontaneous breaking of the O(3) spin symmetry, and this "quantum disordered" regime has gapped spin

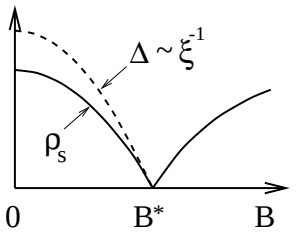

Fig. 2. Schematic behaviour of spin stiffness and correlation length, or spin gap, with applied field.

excitations ($\Delta \propto \xi^{-1}$). For $B > B^*$, the field enforces a quasi-long-ranged correlation throughout the system, the symmetry is lowered to O(2), or XY, and in-plane fluctuations (ϕ in Eq. (3)) are massless. In the 1d model this

is the "quantum critical" phase; in higher dimensions the presence of gapless modes gives the properties of the "renormalised classical" phase of Ref. [2]. Excitation modes (ϑ) in the field direction are gapped with "mass" b. The suppression of quantum fluctuations which leads to this symmetry breaking is the origin of the field-induced quantum phase transition between the two distinct regimes.

2.2. Renormalisation group

Renormalisation-Group (RG) study of the NLσM in an applied field yields meaningful results over the full field range. Application of a standard Wilson momentum–shell treatment to the action of Eq. (2) yields to 1-loop order in the (small) coupling constant g a self-similar form. With flow parameter $l = \ln(a'/a)$, the differential form of the resulting, coupled RG equations is

$$\frac{dg}{dl} = \frac{g^2}{2\pi}\frac{1}{1+\bar{\beta}^2}\,, \tag{6}$$

$$\frac{d\bar{\beta}^2}{dl} = 2\bar{\beta}^2 - \frac{g}{2\pi}\ln\left(1+\bar{\beta}^2\right)\,. \tag{7}$$

These represent an extension of the usual NLσM RG equations to include the magnetic field B, contained in $\bar{\beta} = a' = a'b(a')/c$. Eq. (6) is the conventional "β-equation" for renormalisation of the coupling constant, with an additional field term in the denominator. A strong field restricts flow to the strong-coupling (disordered) limit, effectively suppressing quantum fluctuation effects, and suggesting a "deconfinement of excitations" at suitably high field. Eq. (7) gives renormalisation of the field with dynamical exponent $z = 1$ from the first term, but with additional, logarithmic suppression of this flow at strong field and coupling (second term).

Solution of the RG equations gives the flow diagram in Fig. 3. The regime *(i)* of weak initial B-field is a strong-coupling phase, with confinement of (gapped) excitations. Here, the assumption (underlying the perturbative RG treatment) of small g becomes inconsistent, but the equations contain a physically meaningful cut-off lengthscale $\mathcal{L}_* = a\mathrm{e}^{2\pi/g_0}(\equiv \xi_0)$, where in addition the magnetisation M is zero. In this region O(3) symmetry is restored by quantum fluctuations, which may thereby be considered as "screening" the magnetic field. In contrast, the regime *(ii)* of strong initial B-field corresponds to weak coupling, where g and b/c are only weakly renormalised. Here the excitations are deconfined on a length scale $\bar{\xi}(B)$ whose flow is governed by B. In this region, quantum fluctuations are suppressed by the magnetic field, and the broken O(3) symmetry cannot be restored. The properties of the broken- and unbroken-symmetry phases may be further contrasted by considering physical properties such the correlation length ξ or magnetisation M in each regime [11].

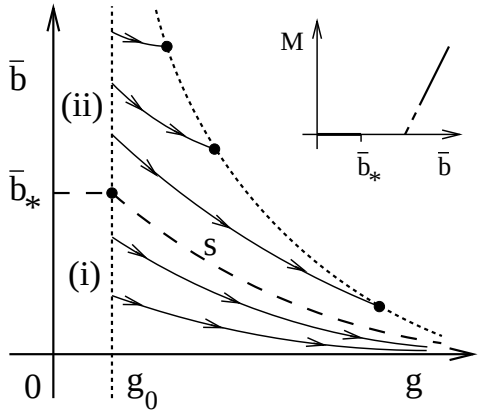

Fig. 3. RG flow diagram for g and $\bar{b}$. Strong- and weak-coupling regimes are separated by separatrix s.

The NLσM treatment may be further employed to compute the magnetisation and critical fields, and extended to calculate spin correlation functions, and decay exponents accessible by NMR experiments. Saturation of the spins, giving rise to a truly classical magnetic system, may be incorporated by a constraint on the uniform component $\boldsymbol{l}$. Comparison to experiment is deferred until Sec. 4, and additional details are contained in Ref. [11]. To summarise this section, the NLσM gives a good qualitative account of the quantum phases of AF systems in an external field, which may be understood on the basis of symmetry-breaking due to the competition of field and quantum fluctuation effects.

3. Quantum phase transitions: bond operators

The NLσM employed in the previous section is unable to provide quantitative information concerning spin gaps or excitations in the quantum phases of the system, or concerning transitions between these phases. To obtain more microscopic insight, one may turn to the bond operator technique, which unlike the NLσM is more restricted in its range of application. The bond-operator method [14] may be applied for any $S = \frac{1}{2}$ spin system with a unique dimer covering, and has been found [15] to give a good description of the two-chain ladder (Fig. 1) for coupling ratios $\lambda = J'/J \leq 1$. It is most appropriate for gapped spin systems, *i.e.* in the "quantum disordered" phase of the canonical phase transition discussion [2]. However, it has also been shown to be applicable to the "renormalised classical" regime, and thus to be a suitable analytical method for quantum phase transitions induced by interladder coupling [16].

Here the bond-operator formalism is extended systematically to finite magnetic fields. It is shown to be a consistent description of all three quantum phases, and hence a most appropriate framework in which to discuss transitions. For a dimer unit in a magnetic field, the eigenstates are linear combinations of the $S_z = 0$ bond operators $t_\alpha^\dagger$ ($\alpha = x, y, z$) of Ref. [14], which represent the spins according to

$$S_{1(2),\alpha} = \tfrac{1}{2}\left[+(-)(s^\dagger t_\alpha + t_\alpha^\dagger s) - i\varepsilon_{\alpha\beta\gamma} t_\beta^\dagger t_\gamma\right], \tag{8}$$

and whose bosonic commutation relations reproduce the SU(2) spin algebra. The new operator combinations are

$$|t_+\rangle = \tfrac{1}{\sqrt{2}}(t_x^\dagger + i t_y^\dagger)|0\rangle \equiv -|\uparrow\uparrow\rangle, \tag{9}$$

$$|t_-\rangle = \tfrac{1}{\sqrt{2}}(t_x^\dagger - i t_y^\dagger)|0\rangle \equiv +|\downarrow\downarrow\rangle, \tag{10}$$

$$|t_0\rangle = t_z^\dagger|0\rangle \equiv \tfrac{1}{\sqrt{2}}(|\uparrow\downarrow\rangle + |\downarrow\uparrow\rangle), \tag{11}$$

whence for terms in the transformation to follow

$$t_x^\dagger t_x + t_y^\dagger t_y = t_+^\dagger t_+ + t_-^\dagger t_-$$

and

$$t_x^\dagger t_x^\dagger + t_y^\dagger t_y^\dagger = t_+^\dagger t_-^\dagger + t_-^\dagger t_+^\dagger, \tag{12}$$

i.e. diagonal terms transform into diagonal ones, but off-diagonal terms transform to mode-mixing ones. A magnetic field term has a diagonal representation

$$-\boldsymbol{b}\cdot(\boldsymbol{S}_1 + \boldsymbol{S}_2) = i b_z\left(t_x^\dagger t_y - t_y^\dagger t_x\right) = b\left(t_+^\dagger t_+ - t_-^\dagger t_-\right), \tag{13}$$

ensuring that the operators $t_{0,\pm1}^\dagger$ reproduce the energy levels of the field eigenstates $S_z = 0, \pm 1$.

Transformation of Eq. (1) into bond operators [14,15] leads to a Hamiltonian with quadratic and quartic terms in operators $(s_i, t_{i\gamma})$, from the rung and chain terms respectively, a quadratic field term, and a constraint term which introduces a chemical potential μ_i to ensure the single occupancy of each dimer i by states $|s_i\rangle$ or $|t_{i\gamma}\rangle$: the bosonic operators have hard-core nature. Treatment of this Hamiltonian follows by a mean-field approximation with retention of quadratic terms, and differs in each of the three regimes of magnetic field.

3.1. $B < B_{c1}$

For magnetic fields below the first critical field B_{c1}, the system is in the quantum disordered regime with a spin gap between the singlet and triplet states on each dimer. In the bond-operator technique this situation is represented [14] by replacing the operator s_i everywhere with its global expectation value $\langle s_i \rangle = \overline{s}$, corresponding to a Bose condensation of the singlet states. Quantum fluctuations about this ground state of pure dimer singlets are contained in the triplet operators $t^{\dagger}_{i\gamma}$, and for a system with strong rung coupling ($\lambda \ll 1$) these are weak (few excited triplets). Replacing also the chemical potential with a global average value $\mu_i = \mu$, the Hamiltonian is [15]

$$\begin{aligned} H &= N(-\tfrac{3}{4}J\overline{s}^2 - \mu\overline{s}^2 + \mu) + \sum_k \left((\tfrac{1}{4}J - \mu \pm b) t^{\dagger}_{k\pm} t_{k\pm} + (\tfrac{1}{4}J - \mu) t^{\dagger}_{k0} t_{k0} \right) \\ &+ \tfrac{1}{2}\lambda J \overline{s}^2 \sum_{k\gamma} \cos k \left(t^{\dagger}_{k\gamma} t_{k\gamma} + t^{\dagger}_{-k\gamma} t_{-k\gamma} + t^{\dagger}_{k\gamma} t^{\dagger}_{-k\overline{\gamma}} + t_{k\gamma} t_{-k\overline{\gamma}} \right) + O(t^4), \end{aligned} \tag{14}$$

where $\overline{\gamma} = -, 0, +$ for modes $\gamma = +, 0, -$. Diagonalisation of the Hamiltonian matrix gives the three modes $\omega_k + b$, ω_k and $\omega_k - b$, where

$$\omega_k = \left[(\tfrac{1}{4}J - \mu)(\tfrac{1}{4}J - \mu + 2\lambda J \overline{s}^2 \cos k) \right]^{1/2} \tag{15}$$

is the dispersion relation for the field-free ladder [15]. The triplet modes do not interact, and are merely split by the magnetic field, as shown in Fig. 4(a). The parameters $\overline{s} = \overline{s}_1$ and $\mu = \mu_1$ are fixed only by the ratio λ, and do not evolve with increasing field below the lower critical field

$$b_{c1} = \left[(\tfrac{1}{4}J - \mu_1)(\tfrac{1}{4}J - \mu_1 + 2\lambda J \overline{s}_1^2 \cos k) \right]^{1/2} = \Delta_0, \tag{16}$$

the zero-field spin gap. The gap is a linearly decreasing function of field in the entire range from 0 to b_{c1}, and the free energy is constant.

3.2. $B > B_{c2}$

In the high-field regime the spins are fully polarised. In bond-operator notation one may represent the ground state as a Bose condensate of the triplet mode $t^{\dagger}_{i-}$ favoured by the field, $\langle t_{i-} \rangle \to \overline{t}$. The quadratic Hamiltonian is

$$\begin{aligned} H &= N(\tfrac{1}{4}J\overline{t}^2 - \mu\overline{t}^2 + \mu) - Nb\overline{t}^2 + \tfrac{1}{2}N\lambda J\overline{t}^4 \\ &+ \sum_k \left(\omega^s_k s^{\dagger}_k s_k + \omega^0_k t^{\dagger}_{k0} t_{k0} + \omega^+_k t^{\dagger}_{k+} t_{k+} \right), \end{aligned} \tag{17}$$

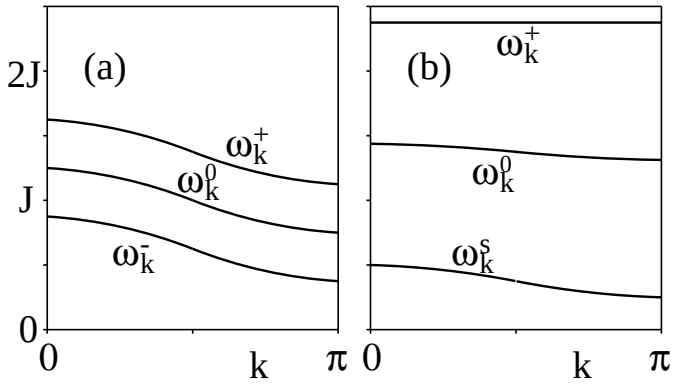

Fig. 4. Magnon dispersion relations for (a) quantum disordered regime $B < B_{c1}$ and (b) fully polarised, classical regime $B > B_{c2}$.

and contains no remaining off-diagonal terms. Solution of the mean-field equation in μ returns the result $\bar{t} = 1$: the polarised system is completely classical in the sense that all quantum fluctuations are suppressed by the field. The magnon energies in Eq. (17) are

$$\omega_k^+ = \tfrac{1}{4}J - \mu - \lambda J + b, \tag{18}$$

$$\omega_k^0 = \tfrac{1}{4}J - \mu + \tfrac{1}{2}\lambda J \cos k\,, \tag{19}$$

$$\omega_k^s = -\tfrac{3}{4}J - \mu + \lambda J \cos k\,, \tag{20}$$

and are depicted in Fig. 4(b). The upper triplet mode becomes completely non-dispersive, while the remaining modes retain their minimum at the point $k = \pi$. Although the system is ferromagnetic, this configuration is enforced by the field, and the lowest-lying excitations remain those of AF nature. These correspond to the action of the spin-raising operator S_i^- in a spin-wave description, which here is completely equivalent. The second mean-field equation gives a condition $\frac{1}{4}J - \mu - b + \lambda J = 0$, showing that μ varies linearly with the field in this regime. In conjunction with the condition $\omega_\pi^s|_{b=b_{c2}} = 0$, that the lowest mode be massless at the transition, one may deduce the upper critical field

$$b_{c2} = J + 2\lambda J\,, \tag{21}$$

which has precisely the value expected classically from the AF couplings to each spin.

3.3. $B_{c1} < B < B_{c2}$

In the intermediate-field regime, the ground state of each dimer can be considered as a partially polarised ferromagnetic configuration, or a canted AF. In the bond-operator formulation, this ordered ground state would be represented by finite expectation values $\overline{s}$ and $\overline{t}$ of both the singlet and t_- triplet operators. However, from these two degrees of freedom there may only be one ground-state condensate, with one gapless fluctuation mode orthogonal to it. The initial states may be written as the sum of a condensed part and a fluctuating component,

$$|s_i\rangle = \overline{s} + |\tilde{s}_i\rangle\,, \quad |t_i\rangle = \overline{t} + |\tilde{t}_{i-}\rangle \tag{22}$$

and transformed according to

$$\begin{pmatrix} |\sigma_i\rangle \\ |\tau_i\rangle \end{pmatrix} = \frac{1}{\sqrt{1+\alpha^2}} \begin{pmatrix} 1 & \alpha \\ -\alpha & 1 \end{pmatrix} \begin{pmatrix} |s_i\rangle \\ |t_{i-}\rangle \end{pmatrix}. \tag{23}$$

The requirement that $|\tau_i\rangle$ be a pure fluctuation mode sets the condition $\alpha = \overline{t}/\overline{s}$. The fluctuating part of $|\sigma_i\rangle$ is then seen to vanish, as it is orthogonal to the sole fluctuation $|\tau_i\rangle$, leaving $|\sigma_i\rangle = \overline{\sigma}_i$ as the Bose condensate. Thus

$$\overline{\sigma}_i = \sqrt{\overline{s}_i^2 + \overline{t}_i^2} \quad \text{and} \quad |\tau_i\rangle = \frac{|\tilde{t}_{i-}\rangle - \alpha|\tilde{s}_i\rangle}{\sqrt{1+\alpha^2}} \tag{24}$$

are the appropriate linear combinations with which to describe the intermediate phase.

The initial Hamiltonian in the intermediate-field regime may now be reexpressed in terms of operators σ_i, τ_i, t_{i0} and t_{i+}. After condensation of σ_i, the three excitation branches separate into a coupled pair and a decoupled mode with dispersion relations

$$\omega_k^+ = \sqrt{{\Lambda_k^+}^2 - \Delta_k^2} + \Lambda_k^-\,, \tag{25}$$

$$\omega_k^0 = \left[\left(\tfrac{1}{4}J - \mu + \tfrac{1}{2}\lambda J\overline{t}^2\cos k\right)\left(\tfrac{1}{4}J - \mu + (\tfrac{1}{2}\lambda J\overline{t}^2 + 2\lambda J\overline{s}^2)\cos k\right)\right]^{1/2}, \tag{26}$$

$$\omega_k^- = \sqrt{{\Lambda_k^+}^2 - \Delta_k^2} - \Lambda_k^-\,, \tag{27}$$

in which $\Lambda_k^{\pm} = \frac{1}{2}\left(\Lambda_k^1 \pm \Lambda_k^2\right)$, and the coefficients

$$\Lambda_k^1 = \tfrac{1}{4}J - \mu + b - \lambda J\overline{t}^2 + \lambda J\overline{s}^2\cos k\,, \tag{28}$$

$$\Lambda_k^2 = \tfrac{1}{4}J - \mu - b + \frac{\overline{t}^2(b-J) + \lambda J\overline{s}^2\overline{t}^2 + \lambda J\cos k(\overline{s}^4 + \overline{t}^4)}{\overline{s}^2 + \overline{t}^2}\,, \tag{29}$$

$$\Delta_k = \lambda J\cos k\frac{\overline{s}^3}{\sqrt{\overline{s}^2 + \overline{t}^2}} \tag{30}$$

allow one to make contact with previous results [15,16]. The $S_z = 0$ branch, ω_k^0, remains independent of the magnetic field, while the coupled branches, $\omega_k^{\pm}$, are field-dependent. The most important feature of these mode energies is that they interpolate smoothly from the forms in the low- and high-field regimes when $\overline{t}$ and $\overline{s}$, respectively, are taken to zero at the phase transitions b_{c1} and b_{c2}. The dispersion relations are shown in Fig. 5(a).

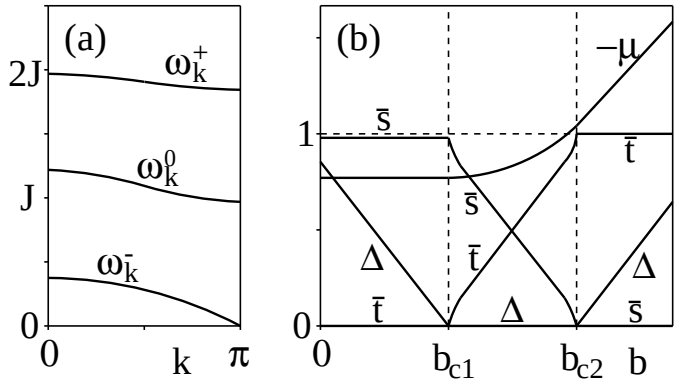

Fig. 5. (a) Magnon dispersion relations in quantum critical regime $B_{c1} < B < B_{c2}$. (b) Evolution with field b of order parameters $\overline{s}$ and $\overline{t}$, chemical potential μ and spin gap Δ over the field range spanning all three quantum phases.

The quadratic Hamiltonian in the intermediate-field regime is then

$$\begin{aligned} H \;=\; & N\Big[(-\tfrac{3}{4}J-\mu)\overline{s}^2+(\tfrac{1}{4}J-\mu)\overline{t}^2+\mu-b\overline{t}^2+\lambda J\overline{s}^2\overline{t}^2+\tfrac{1}{2}\lambda J\overline{t}^4 \\ & -\tfrac{1}{2}(\tfrac{1}{4}J-\mu)-\tfrac{1}{2}(\tfrac{1}{4}J-\mu+b-\lambda J\overline{t}^2) \\ & -\tfrac{1}{2}\left(\tfrac{1}{4}J-\mu-b+\left(\overline{t}^2(b-J)+\lambda J\overline{s}^2\overline{t}^2\right)/(\overline{s}^2+\overline{t}^2)\right)\Big] \\ & +\sum_k\Big[\omega_k^-\left(\tilde{\tau}_k^\dagger\tilde{\tau}_k+\tfrac{1}{2}\right)+\omega_k^0\left(t_{k0}^\dagger t_{k0}+\tfrac{1}{2}\right)+\omega_k^+\left(\tilde{t}_{k+}^\dagger\tilde{t}_{k+}+\tfrac{1}{2}\right)\Big]. \end{aligned} \tag{31}$$

Minimisation of the corresponding zero-temperature free energy gives the self-consistent solutions for the order parameters $\overline{s}$ and $\overline{t}$ for all values of the field. This minimisation is performed subject to the physical constraint that $\omega_\pi^- = 0$, *i.e.* that the lowest excitation mode be massless throughout this field regime, as in Fig. 5(a). The gapless excitation mode is the defining feature of the physics at intermediate fields, and the application of the physical constraint represents a partially-controlled means of taking the treatment beyond quadratic order [16]. As noted above, the dispersion minimum always occurs at $k = \pi$, and there are no incommensurate excitations in the bond-operator construction.

The solutions for $\overline{s}$ and $\overline{t}$ quantify the picture of a partially polarised magnetic state on every rung. The deviation of $(\overline{s}^2 + \overline{t}^2)$ from unity can be taken to characterise the effect of quantum fluctuations, and shows as in the previous section that increasing field suppresses these (completely at B_{c2}). The field tunes the system from a quantum, dimerised phase to a classical, ordered one.

After this analysis, the issue of quantum phase transitions is easy to study in such a unified framework for all three phases: the continuity of all properties at the phase boundaries ensures second-order transitions, and one may consider further the critical exponents of static and dynamic quantities around the critical points. The most important of these is that the magnetisation $M \propto \overline{t}^2$ [16] is expected to have the field dependence $M \propto \sqrt{b - b_{c1}}$ as $b \to b_{c1}$ from above, and $M \propto \sqrt{b_{c2} - b}$ as $b \to b_{c2}$ from below. In the bond-operator description for small λ, where quantum fluctuations are always small, these square-root regimes are found to be rather narrow (Fig. 5(b)).

To conclude this part of the discussion, the bond-operator approach is particularly suitable for the strongly dimerised system CuHpCl, and in fact renders quantum fluctuation effects beyond the singlet ground state rather small even in the "quantum disordered" regime. The method gives a microscopic description of the ground states and excitations in all three phases. Most importantly, the unified formulation across the full field range makes this technique uniquely suitable for discussing the quantum phase transitions, which by suitable choice of the condensate are quite straightforward found to be continuous. The bond-operator formalism is readily extended to higher-dimensional problems, alternating chains and systems with frustrating couplings, subject to the requirement that the geometry allow a unique dimerisation.

4. Experiment

Specialising to the parameters of CuHpCl, the NLσM approach requires the exchange constants deduced from magnetisation and susceptibility measurements [3, 4], $J/k_{\rm B} = 13.2$ K and $J'/k_{\rm B} = 2.4$ K, whence $B_{c1} = 6.6$ T and $B_{c2} = 13.3$ T [11]. The bond-operator technique allows an independent fit to the data, from which the deduced zero-temperature critical fields, $B_{c1} = 7.1$ T and $B_{c2} = 13.6$ T, give the exchange constants $J/k_{\rm B} = 12.5$ K and $J'/k_{\rm B} = 2.9$ K. The bond-operator coupling ratio is then $\lambda = 0.23$. The results of these fits are shown in Fig. 6; both give the same, predominantly linear magnetisation observed in experiment, which however is not in full accord with numerical simulations of the minimal model [7,10].

The other category of experiments performed on CuHpCl is the measurement of NMR spin relaxation rates, which probe spin–spin correlation

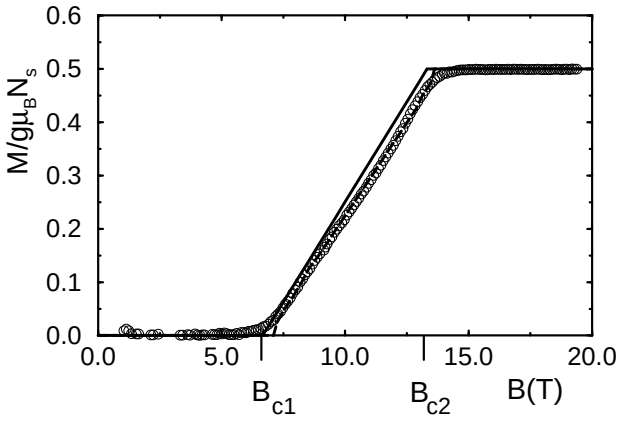

Fig. 6. Magnetisation calculated for the spin ladder system CuHpCl by the NLσM (solid) and bond-operator (dashed) techniques. Circles are data from Ref. [3].

functions. These have been computed within the NLσM [11], and using bond operators for a coupled ladder system [16]. Because the experimental data allow only qualitative conclusions concerning the presence and magnitude of the spin gap, and cannot be used to compare exponents, these quantities will not be discussed further here. The two methods give a good account of available experimental data concerning the quantum phases and their boundaries, which are summarised in the phase diagram of Ref. [17], albeit with one major exception. This is the presence of a 3d ordered phase within the gapless, intermediate-field regime. Such a phase is expected in the presence of any higher-dimensional couplings, however weak, as these will constitute relevant perturbations of the ground state in the quantum critical phase. The bond-operator technique permits a description of this phase in terms of a condensate formed by linear combination of three components with finite expectation values, $\langle s_i \rangle$, $\langle t_{i0} \rangle$ and $\langle t_{i-} \rangle$, from the singlet, $S_z = 0$ triplet and high-field triplet modes. However, the presence of a spin gap in the excitation spectrum, observed recently in this regime [17], does come as a surprise, and similarly requires additional terms beyond the model considered here. While a form of phonon coupling, or spin-Peierls phenomenon, has been proposed [17] to account for this result within the spin-ladder framework (1), recent indications from inelastic neutron scattering [18] raise the possibility that an alternative model description may in fact be necessary for CuHpCl.

5. Summary

The quantum antiferromagnet in a magnetic field provides an ideal illustration of quantum phases in different universality classes, of symmetry-breaking, and of quantum phase transitions. A NLσM description contains at low but finite fields the restoration of O(3) symmetry of the spin Hamiltonian by strong quantum fluctuations, the effect of "asymptotic freedom". Fields which are sufficiently strong, but remain experimentally accessible in materials such as CuHpCl, suppress quantum fluctuations such that the spin system is reduced to the lower O(2) (XY) symmetry. In this case there are gapless excitation modes and no true long range order, but instead a quasi-long-range order characterised by spin–spin correlation functions which decay in space and time with a power law form. A bond-operator description contains the microscopic picture of these phases in terms of singlet and triplet excitations on each dimer bond of the appropriate lattice structure. The eigenstates of wavevector and field have the same gapped and gapless properties as the NLσM phases, and interpolate continuously across the entire field range. This consistent description is uniquely suitable for the study of quantum phase transitions, which are second-order in nature.

The author wishes to thank G. Chaboussant, L. Lévy, D. Loss, F. Mila, D. Reich, T.M. Rice and G. Sierra for helpful discussions, and is especially grateful to J. Dukelsky for invaluable insight into the treatment of the bond-operator condensate. This work was supported by Treubelfonds, and by the Deutsche Forschungsgemeinschaft through SFB 484.

REFERENCES

[1] F.D.M. Haldane, *Phys. Lett.* **93A**, 464 (1983); *Phys. Rev. Lett.* **50**, 1153 (1983).

[2] S. Chakravarty, B.I. Halperin, D.R. Nelson, *Phys. Rev.* **B39**, 2344 (1989).

[3] G. Chaboussant, P.A. Crowell, L.P. Lévy, O. Piovesana, A. Madouri, D. Mailly, *Phys. Rev.* **B55**, 3046 (1997).

[4] P.R. Hammar, D.H. Reich, C. Broholm, F. Trouw, *Phys. Rev.* **B57**, 7846 (1998).

[5] G. Chaboussant, Y. Fagot-Revurat, M.-H. Julien, M.E. Hanson, C. Berthier, M. Horvatic, L.P. Lévy, O. Piovesana, *Phys. Rev. Lett.* **80**, 2713 (1998).

[6] G. Chaboussant, M.-H. Julien, Y. Fagot-Revurat, M.E. Hanson, L.P. Lévy, C. Berthier, M. Horvatic, O. Piovesana, *Eur. Phys. J.* **B6**, 167 (1998).

[7] C.A. Hayward, D. Poilblanc, L.P. Lévy, *Phys. Rev.* **B54**, R12649 (1996).

[8] R. Chitra, T. Giamarchi, *Phys. Rev.* **B55**, 5819 (1997).

[9] F. Mila, *Eur. Phys. J.* **B6**, 201 (1998).

[10] X. Wang, Yu Lu, *Phys. Rev. Lett.* **84**, 5399 (2000).

[11] B. Normand, J. Kyriakidis, D. Loss, *Ann. Phys.* (Leipzig), **9**, 133 (2000).

[12] H.J. Mikeska, *J. Phys. C* **13**, 2913 (1980); A.F. Andreev, V.I. Marchenko, *Sov. Phys. Usp.* **23**, 21 (1980).

[13] D. Loss, D.L. Maslov, *Phys. Rev. Lett.* **74**, 178 (1995).

[14] S. Sachdev, R. Bhatt, *Phys. Rev.* **B41**, 9323 (1990).

[15] S. Gopalan, T.M. Rice, M. Sigrist, *Phys. Rev.* **B49**, 8901 (1994).

[16] B. Normand, T.M. Rice, *Phys. Rev.* **B56**, 8760 (1997).

[17] H. Mayaffre, M. Horvatic, C. Berthier, M.-H. Julien, P. Ségransan, L.P. Lévy, O. Piovesana, unpublished.

[18] D.H. Reich, unpublished.